Available online at www.sciencedirect.com
ScienceDirect
Biochemical and Biophysical Research Communications 366 (2008) 186–192
BBRC
www.elsevier.com/locate/ybbrc

Comparative proteomic and transcriptomic profiling of the human hepatocellular carcinoma

Hirotaka Minagawa [a], Masao Honda [b,*], Kenji Miyazaki [c], Yo Tabuse [c,*], Reiji Teramoto [c], Taro Yamashita [b], Ryuhei Nishino [b], Hajime Takatori [b], Teruyuki Ueda [b], Ken'ichi Kamijo [a], Shuichi Kaneko [b]

[a] *Nano Electronics Research Laboratories, NEC Corporation, 34, Miyukigaoka, Tsukuba, Ibaraki 305-8501, Japan*
[b] *Department of Gastroenterology, Kanazawa University Graduate School of Medical Science, Kanazawa, 13-1 Takara-machi, Kanazawa 920-8641, Japan*
[c] *Bio-IT Center, NEC Corporation, 34, Miyukigaoka, Tsukuba, Ibaraki 305-8501, Japan*

Received 14 November 2007
Available online 4 December 2007

Abstract

Proteome analysis of human hepatocellular carcinoma (HCC) was done using two-dimensional difference gel electrophoresis. To gain an understanding of the molecular events accompanying HCC development, we compared the protein expression profiles of HCC and non-HCC tissue from 14 patients to the mRNA expression profiles of the same samples made from a cDNA microarray. A total of 125 proteins were identified, and the expression profiles of 93 proteins (149 spots) were compared to the mRNA expression profiles. The overall protein expression ratios correlated well with the mRNA ratios between HCC and non-HCC (Pearson's correlation coefficient: $r = 0.73$). Particularly, the HCC/non-HCC expression ratios of proteins involved in metabolic processes showed significant correlation to those of mRNA ($r = 0.9$). A considerable number of proteins were expressed as multiple spots. Among them, several proteins showed spot-to-spot differences in expression level and their expression ratios between HCC and non-HCC poorly correlated to mRNA ratios. Such multi-spotted proteins might arise as a consequence of post-translational modifications.

Keywords: Hepatocellular carcinoma; Proteome; Two-dimensional difference gel electrophoresis; Transcriptome; cDNA microarray

Hepatocellular carcinoma (HCC) is one of the most common cancers worldwide, and a leading cause of death in Africa and Asia [1]. Although several major risks related to HCC, such as hepatitis B and/or hepatitis C virus infection, aflatoxin B1 exposure, and alcohol consumption, and genetic defects, have been revealed [2], the molecular mechanisms leading to the initiation and progression of HCC are not well known. To find the molecular basis of hepatocarcinogenesis, comprehensive gene expression analyses have been done using many systems such as hepatoma cell lines and tissue samples [3,4]. Previously, we have carried out a comprehensive mRNA expression analysis using the serial analysis of gene expression (SAGE) [5] and cDNA microarray-based comparative genomic hybridization [6] to acquire the outline of gene expression profile of HCC. Although these genomic approaches have yielded global gene expression profiles in HCC and identified a number of candidate genes as biomarkers useful for cancer staging, prediction of prognosis, and treatment selection [7], the molecular events accompanying HCC development are not yet understood. In general, proteins rather than transcripts are the major effectors of cellular and tissue function [8] and it is accepted that protein expression do not always correlate with mRNA expression [9,10]. Thus, protein expression analysis, which could complement the available mRNA data, is also important to understand the molecular mechanisms of HCC.

* Corresponding authors. Fax: +81 76 234 4250 (M. Honda), +81 29 856 6136 (Y.Tabuse).
E-mail addresses: mhonda@medf.m.kanazawa-u.ac.jp (M. Honda), y-tabuse@cd.jp.nec.com (Y. Tabuse).

0006-291X/$ - see front matter © 2007 Elsevier Inc. All rights reserved.
doi:10.1016/j.bbrc.2007.11.101

The technique of two-dimensional difference gel electrophoresis (2D-DIGE), developed by Unlu et al. [11] is one of major advances in quantitative proteomics. Several groups have recently utilized 2D-DIGE to examine protein expression changes in HCC samples [12,13], whereas reports on the analysis combining both transcriptomic and proteomic approach are rare.

In the present study, we compared quantitatively protein expression profiles of HCC to non-HCC (non-cancerous liver) samples derived from 14 patients by 2D-DIGE. We also compared the protein expression profiles of the same HCC and non-HCC samples to the mRNA profiles which have been obtained using a cDNA microarray. The expression ratios of 93 proteins showed significant correlations with the mRNA ratios between HCC and non-HCC. Proteins involved in metabolic processes showed more prominent correlation. Our study describes an outline of gene and protein expression profiles in HCC, thus providing us a basis for better understanding of the disease.

Materials and methods

Patients. A total of 14 HCC patients who had surgical resection done in the Kanazawa University Hospital were enrolled. The clinicopathological characteristics of them are shown in Table 1. The HCC samples and adjacent non-tumor liver samples were snap frozen in liquid nitrogen, and used for cDNA microarray and 2D-DIGE analysis. All HCC and non-tumor samples were histologically diagnosed and quantitative detection of hepatitis C virus RNA by Amplicore analysis (Roche Diagnostic Systems) showed positive. The grading and staging of chronic hepatitis associated with non-tumor lesion were histologically assessed according to the method described by Desmet et al. [14] and histological typing of HCC was assessed according to Ishak et al. [15]. All strategies used for gene expression and protein expression analysis were approved by the Ethical Committee of Kanazawa University Hospital.

Preparation of cDNA microarray slides. In addition to in-house cDNA microarray slides consisting of 1080 cDNA clones as previously described [6,16–18], we made new cDNA microarray slides for detailed analysis of the signaling pathway of metabolism and enzyme function in liver disease [19]. Besides cDNA microarray analysis, a total of 256,550 tags were obtained from hepatic SAGE libraries (derived from normal liver, CH-C, CH-C related HCC, CH-B, and CH-B related HCC), including 52,149 unique tags. Among these, 16,916 tags expressing more than two hits were selected to avoid the effect of sequencing errors in the libraries. From these candidate genes, 9614 non-redundant clones were obtained from Incyte Genomics (Incyte Corporation), Clontech (Nippon Becton Dickinson), and Invitrogen (Invitrogen). Each clone was sequence validated and PCR amplified by Dragon Genomics (Takara Bio), and the cDNA microarray slides (Liver chip 10k) were constructed using SPBIO 2000 (Hitachi Software) as described previously [6,16–18].

Table 1
Characteristics of patients involved in this study

Patient No.	Age	Sex[a]	Histology of non-tumor lesion[b]	Tumor histology	Viral status
1	64	M	F4A1	Moderate	HCV
2	65	M	F4A1	Well	HCV
3	48	M	F3A1	Moderate	HCV
4	69	F	F4A2	Moderate	HCV
5	66	F	F4A2	Well	HCV
6	45	M	F4A1	Well	HCV
7	75	F	F4A1	Well	HCV
8	46	M	F4A2	Moderate	HCV
9	66	M	F2A2	Well	HCV
10	75	M	F3A1	Moderate	HCV
11	67	F	F4A2	Well	HCV
12	64	M	F4A1	Moderate	HCV
13	68	M	F4A0	Well	HCV
14	74	M	F1A0	Moderate	HCV

[a] M, male; F, female.
[b] F, fibrosis; A, activity.

RNA isolation and antisense RNA amplification. Total RNA was isolated from liver biopsy samples using an RNA extraction kit (Stratagene). Aliquots of total RNA (5 μg) were subjected to amplification with antisense RNA (aRNA) using a Message AmpTM aRNA kit (Ambion) as recommended by the manufacturer. About 25 μg of aRNA was amplified from 5 μg total RNA, assuming that 500-fold amplification of mRNA was obtained. The quality and degradation of the isolated RNA were estimated after electrophoresis using an Agilent 2001 bioanalyzer. In addition, 10 μg of aRNA was used for further labeling procedures.

Hybridization on cDNA microarray slides and image analysis. As a reference for each microarray analysis, aRNA samples prepared from the normal liver tissue from one of the patients were used. Test RNA samples fluorescently labeled with cyanine (Cy) 5 and reference RNA labeled with Cy3 were used for microarray hybridization as described previously [6,16–18]. Quantitative assessment of the signals on the slides was done by scanning on a ScanArray 5000 (General Scanning) followed by image analysis using GenePix Pro 4.1 (Axon Instruments) as described previously [6,16–18].

Protein expression analysis using 2D-DIGE. Protein samples were homogenized with lysis buffer (7 M urea, 2 M thiourea, 4% w/v CHAPS, 0.8 μM aprotinin, 15 μM pepstatin, 0.1 mM PMSF, 0.5 mM EDTA, 30 mM Tris–HCl, pH 8.5) and centrifuged at 13,000 rpm for 20 min at 4 °C. The supernatants were used as protein samples. The protein concentrations were determined with a protein assay reagent (Bio-Rad). The non-HCC and HCC samples (50 μg each) labeled with either Cy3 or Cy5 according to the manufacture's manual were combined and separated on 2-DE gels together with the Cy2-labeled internal standard (IS), which was prepared by mixing equal amounts of all samples. Analytical 2-DE was performed as described previously [20] using Immobiline DryStrip (pH 3–10, 24 cm, GE Healthcare) in the first dimension and 12.5% SDS–polyacrylamide gels (24 × 20 cm) in the second dimension. Samples were run in triplicate to obtain statistically reasonable results. After scanning with a Typhoon 9410 scanner (GE Healthcare), gels were silver stained for protein identification. For protein identification, 400 μg of the IS sample was also separately run on a 2-DE gel and stained with SYPRO Ruby (Invitrogen). All analytical and preparative gel images were processed using ImageQuant (GE Healthcare) and the protein level analysis was done with the DeCyder software (GE Healthcare). To detect phosphoproteins, 400 μg of HCC and non-HCC samples were separately run on 2-DE gels and stained with ProQ Diamond (Invitrogen). After acquiring images, gels were counterstained with SYPRO Ruby to visualize total proteins as described above.

Protein identification. The excised protein spots were in-gel digested with porcine trypsin (Promega). For LC-ESI-IT MS/MS analysis using LCQ Deca XP (Thermo Electron), the digested and dried peptides were dissolved in 10 μl of 0.1% formic acid in 2% acetonitrile (ACN). The dissolved samples were loaded onto C18 silica gel capillary columns (Magic C18, 50 × 0.2 mm), and the elution from the column was directly connected through a sprayer to an ESI-IT MS. Mobile phase A was 2% ACN containing 0.1% formic acid, and mobile phase B was 90% ACN containing 0.1% formic acid. A linear gradient from 5% to 65% of concentration B was applied to elute peptides. The ESI-IT MS was operated in positive ion mode over the range of 350–2000 (m/z) and the database search was carried out against the IPI Human using MASCOT (Matrixscience). The following search parameters were used: the cutting enzyme, trypsin; one missed cleavage allowed, mass tolerance window, ±1 Da, the MS/MS tolerance window, ±0.8 Da; carbamidomethyl cystein and oxidized methionine as fixed and variable modifications, respectively.

Detection of phosphorylated peptide. Possible phosphorylation sites were investigated by MALDI–TOF–MS using monoammonium phosphate (MAP) added matrix mainly according to Nabetani et al. [21]. An additive of MAP was mixed with α-CHCA matrix solution (5 mg/mL, 0.1% TFA, 50% ACN aqueous) to 40 mM in final concentration. Tryptsin digests of the spots positively stained with ProQ were dissolved into 4 μL of 0.1% TFA, 50% ACN aqueous solution and 1 μL of the peptides solution was spotted on the MALDI target plate. After drying up, 1 μL of the MAP matrix was dropped on the dried peptide mixture. Voyager DE-STR (ABI) was used to obtain mass spectra both in negative and positive ion mode. MS peaks that had relatively stronger intensities in negative ion mode than in positive ion mode were selected as candidates for acidically modified peptides.

Results and discussion

We identified 195 spots representing 125 proteins (Suppl. Table 1) and obtained the corresponding mRNA expression data for a total of 93 proteins (149 spots) (Suppl. Table 2). These 93 proteins were classified according to their biological processes and subcellular localizations into categories described by the Gene Ontology Consortium (http://www.geneontology.org/index.shtml) and about a half of them were related to metabolic processes (Fig. 1A). It is a general agreement that proteins with extremely high or low p*I* as well as hydrophobic proteins are difficult to be detected by 2-DE. Being consistent with this notion, our analysis detected many cytoplasmic proteins (Fig. 1B). Therefore, the protein expression data presented here were biased in favor of cytoplasmic and soluble proteins. The protein expression abundance between non-HCC and HCC was calculated using the normalized spot volume, which was the ratio of spot volume relative to IS (Cy3:Cy2 or Cy5:Cy2) and we used the Student's paired *t*-test ($p < 0.05$) to select the protein spots which were expressed differentially between non-HCC and HCC, using 2-DE gel images run in triplicate. The spot volume of a multi-spotted protein was indicated as a total volume by integrating the intensities of multiple spots as was done by Gygi et al. [10]. Comparison of protein expression profiles revealed that several proteins were expressed differentially between HCC and non-HCC. Proteins whose abundances increased >2-fold or decreased <1/2 in HCC are listed in Table 2. While glutamine synthetase, vimentin, annexin A2 and aldo-keto reductase were up-regulated, carbonic anhydrase 2, argininosuccinate synthetase 1, carbonic anhydrase 1, fructose-1,6-bisphosphatase 1, and betaine-homocysteine methyltransferase were down-regulated in HCC. Up- or down-regulation of most of these proteins in HCC has been reported previously [22–27]. Up-regulation of vimentin and annexin A2, and reduced expression of carbonic anhydrase 1 and 2 was suspected to be associated with cellular motility and metastasis [23,24,26].

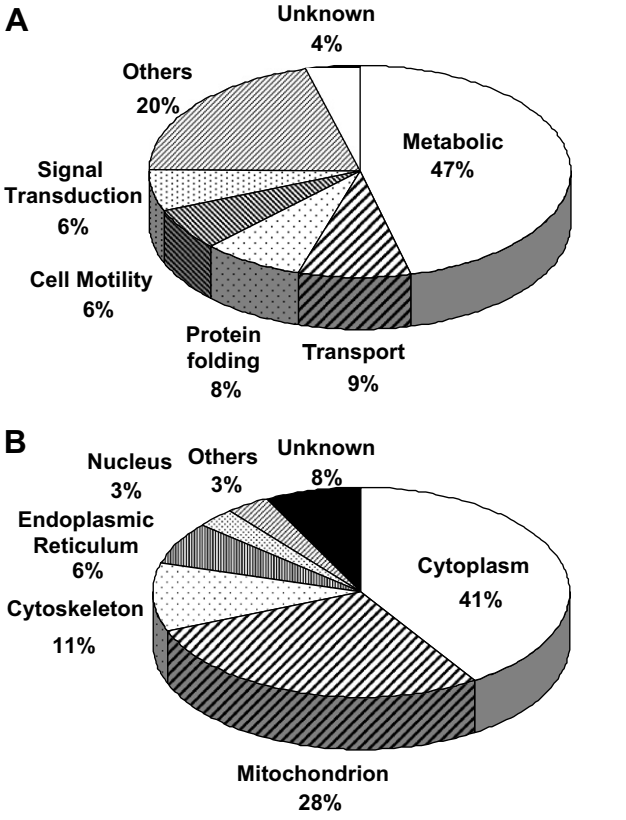

Fig. 1. Classification of identified proteins according to their cellular function (A) and subcellular localization (B).

The mRNA expression abundance was calculated from cDNA microarray data. Hierarchical clustering of

Table 2
Proteins expressed differentially between HCC and non-HCC

Spot ID	Protein name	Refseq ID	Theoretical		Fold change (HCC/non-HCC)		References
			p*I*	MW (kDa)	Protein[a]	mRNA	
1353, 1354	Glutamine synthase	NP_002056.2	6.43	42.7	2.06	3.08	[22]
1039, 1046	Vimentin	NP_003371	5.09	53.6	2.30	1.51	[23]
1716	Annexin A2	NP_001002857.1	7.57	38.8	2.57	1.82	[24]
1685, 1699	Aldo-keto reductase 1B10	NP_064695	7.12	36.2	4.29	4.73	[25]
1977	Carbonic anhydrase 2	NP_000058	6.87	29.3	0.39	0.62	[26]
1307, 1312, 1331	Argininosuccinate synthetase 1	NP_000041.2	8.08	46.8	0.41	0.30	[27]
1941	Carbonic anhydrase 1	NP_001729	6.59	28.9	0.47	1.25	[26]
1582	Fructose-1,6-bisphosphatase 1	NP_000498	6.54	37.2	0.48	0.36	
1256	Betaine-homocysteine methyltransferase	NP_001704	6.41	45.4	0.48	0.40	

[a] Integrated spot volume was used to calculate the fold change of multi-spotted proteins.

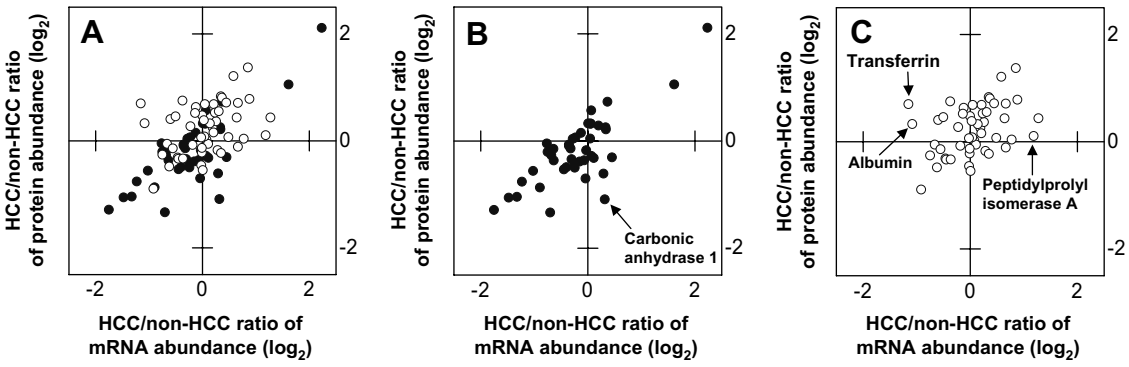

Fig. 2. Comparative analysis of protein and mRNA expression profiles between HCC and non-HCC. (A) The HCC/non-HCC ratios of averaged protein expression levels for 93 proteins were plotted against those of mRNA. Proteins related to metabolic pathways were indicated in closed circles and were shown again in (B). Proteins related to the other biochemical pathways were indicated in open circles and shown in (C). Proteins listed in Table 3 were indicated in (B) and (C). All graphs were depicted in $\log_2$ scale.

Table 3
Proteins whose expression changes between HCC and non-HCC show poor correlation to mRNA expression changes

Spot ID	Protein name	Refseq ID	Theoretical		Spot[a] Av. Ratio	Spot *p* value	Protein ratio	Micro array Av. ratio	Micro array *p* value
			p*I*	MW (kDa)					
564	Transferrin	NP_001054	6.8	79.3	2.23	0.035	1.61	0.45	3.3E−06
565					1.87	0.079			
566					2.28	0.13			
605					0.73	0.098			
1489	Albumin	NP_000468	5.9	71.3	—	0.63	1.25	0.47	2.3E−03
1941	Carbonic anhydrase 1	NP_001729	6.6	28.9	—	3.5E−03	0.47	1.25	0.39
2290	Peptidylprolyl isomerase A	NP_066953	7.7	18.1	—	5.0E−01	1.07	2.29	1.1E−01

[a] Since transferrin was detected in multiple spots, averaged ratio and spot *p* value of each spot is shown.

Table 4
Multi-spotted proteins showing spot-to-spot differences in expression level between non-HCC and HCC

Spot ID	Spot Av. ratio	Spot *p* value	Protein name	Refseq ID	Theoretical		Protein[a] ratio
					p*I*	MW (kDa)	
436	1.92	5.3E−04	Tumor rejection antigen (gp96)	NP_003290	4.8	92.7	1.2
537	0.79	0.16					
564	2.23	0.035	Transferrin	NP_001054	6.8	79.3	1.61
565	1.87	0.079					
566	2.28	0.13					
605	0.73	0.098					
1257	1.02	0.92	Fumarate hydratase	NP_000134	8.8	54.8	0.8
1261	0.6	1.3E−03					

[a] HCC/non-HCC protein ratios were calculated using integrated spot abundances.

gene expression was done with BRB-ArrayTools (http://linus.nci.nih.gov/BRB-ArrayTools.htm). The filtered data were log-transferred, normalized, centered, and applied to the average linkage clustering with centered correlation. BRB-ArrayTools contains a class comparison tool based on univariate *F* tests to find genes differentially expressed between predefined clinical groups. The permutation distribution of the *F* statistic, based on 2000 random permutations, was also used to confirm statistical significance. A *p* value of less than 0.05 for differences in HCC/non-HCC gene expression ratio was considered significant.

The average HCC/non-HCC expression ratios of the 93 proteins were plotted against the mRNA ratios in Fig. 2, where a positive value indicates increased expression in HCC and a negative ratio indicates reduced expression. The overall expression ratio of HCC/non-HCC indicated noticeable correlation between protein and mRNA

(Fig. 2A), and the Pearson's correlation coefficient for this data set (93 proteins/genes) was 0.73. Next, we divided 93 proteins into those related to metabolism and others biological processes. The HCC/non-HCC ratios of protein expression for metabolism-related proteins showed substantial correlation with those of mRNA (Fig. 2B, $r = 0.9$), whereas those of other proteins were poorly correlated (Fig. 2C, $r = 0.36$). Extreme care must be taken in a direct comparison of proteomic data with transcriptome because of multiple layers of discrepancies caused by the distinct sensitivities of cDNA array hybridization and 2-DE, the inability of a cDNA array to distinguish mRNA isoforms and post-translational modifications of proteins. Nevertheless, our results suggest that the expression of considerable portion of proteins with metabolic function listed here is regulated at transcriptional level. On the other hand, post-transcriptional and/or post-translational processes seem to be involved in the regulation of expression level for proteins with other cellular functions as a whole. Four proteins (albumin, transferrin, peptidylproryl isomerase A, and carbonic anhydrase 1) showed apparent poor correlation in protein and mRNA expression profiles (Table 3 and Fig. 2). Transcriptional control might have little effect on the expression changes of these proteins between HCC and non-HCC.

A number of proteins were expressed as multiple spots on 2-DE gels and most multi-spotted proteins showed little spot-to-spot variations in the averaged HCC/non-HCC ratio. Although we do not know how these multiple spots were generated, many of them might be due to the conformational equilibrium of proteins under electrophoresis rather than to any post-translational modifications [28]. On the other hand, the HCC/non-HCC expression ratios of several multi-spotted proteins varied from spot to spot, and three proteins (transferrin, fumarate hydratase, and tumor rejection antigen gp96) were categorized as these multi-spotted proteins (Table 4).

For example, gp96 was detected in two spots (spot #436 and 537) with distinct molecular mass and p*I* and they showed different HCC/non-HCC expression ratio (Fig. 3A and B and Table 4). The expression of these two isoforms was observed to change in the opposite direction between non-HCC and HCC: #436 was up-regulated in HCC (HCC/non-HCC ratio: 1.96) while #537 was down-regulated (HCC/non-HCC ratio: 0.79) (Table 4 and Fig. 3C and D). Gp96 is a glycoprotein present in endoplasmic reticulum and is supposed to function as a molec-

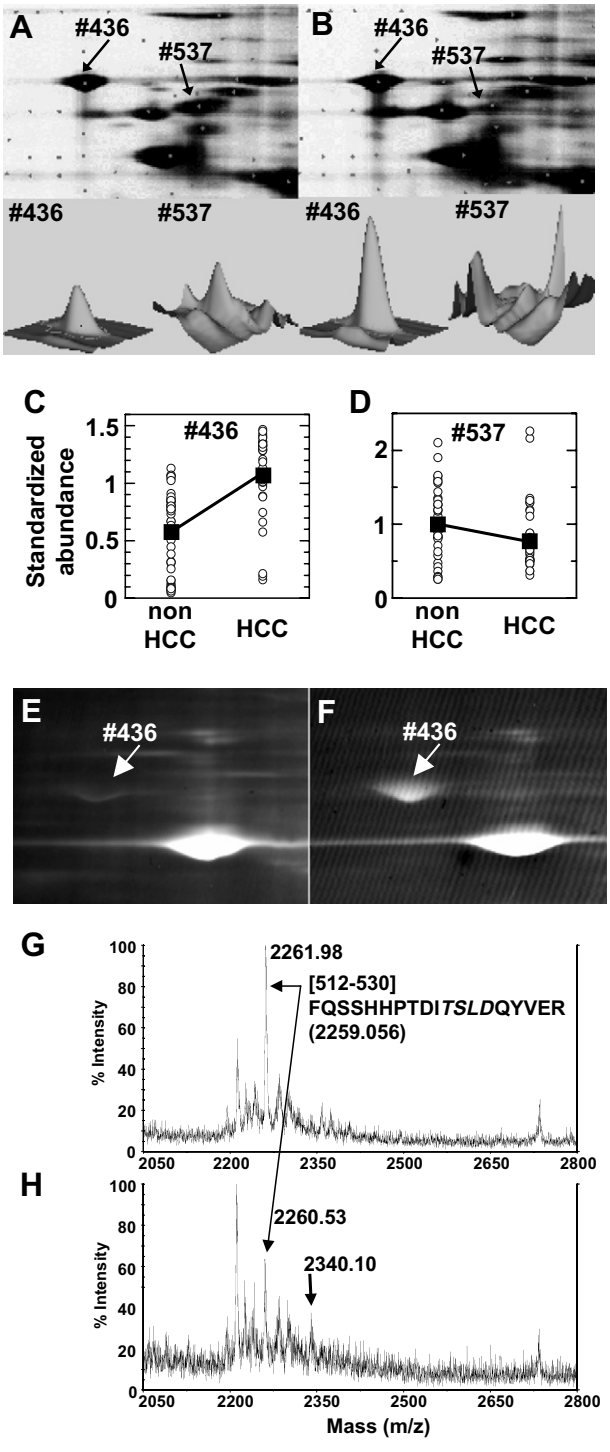

Fig. 3. Comparison of expression profiles of two gp96 spots between HCC and non-HCC. The expression profile and phosphorylation of tumor rejection antigen gp96 in HCC and non-HCC was investigated. Magnified gel images and 3D views of two gp96 spots in non-HCC (A) and HCC (B) were shown. Differences in expression level of two gp96 spots, #436 (C) and #537 (D), between non-HCC and HCC were shown. The open circle indicates the standardized abundance of the individual spot in each sample. The closed square represents the averaged abundance of each gp96 spot. Magnified gel images of non-HCC (E) and HCC (F) stained with ProQ. The #436 spot was positively stained with ProQ, while unambiguous staining of the #537 spot was not observed. Tryptic peptides prepared from the spot #436 were analyzed by MALDI–TOF mass-spectrometry in the positive ion mode (G) and the negative ion mode (H). A peak of 2261.98 detected in positive ion mode corresponds to the amino acid sequence from 512 to 530. In addition to the original peak (*m*/*z*: 2260.53), a peak mass shifted by +80 Da was detected in the negative ion mode. A predicted phosphorylation consensus motif for protein kinase CK2 is indicated in italics (G).

ular chaperone and intracellular Ca^{2+} regulator [29,30]. Several previous reports have shown that gp96 is glycosylated and phosphorylated, and exists as heterogeneous molecular entities with various molecular weights [31]. In order to know whether gp96 spots were phosphorylated or not, we stained the 2-DE gels with ProQ Diamond which is a dye specific to proteins phosphorylated on serine, threonine or tyrosine residues [32], and has been used successfully to visualize phosphoproteins [33]. We found that the spot #436 was positively stained with ProQ (Fig. 3E and F). We further tried to detect possible phosphorylated peptides in the tryptic digests prepared from #436 by MALDI–TOF–MS according to Nabetani et al. [21]. Searching for those peaks that had relatively stronger intensities in negative ion mode than in positive ion mode, we found two peaks as candidates for acidically modified peptides. They were assigned to the peptides SILFVPTSAPR (amino acid sequence: 385–395, data not shown) and FQSSHHPTDITSLDQYVER (aa512–530). Fig. 3G and H show the unmodified peak and the acidically modified peak (mass shifted by +80 Da in negative ion mode) of the latter peptide, respectively. This peptide contained a predicted phosphorylation consensus motif, [Ser or Thr]-X-X-[Asp or Glu], for protein kinase CK2 (Fig. 3G) which was suggested to phosphorylate gp96 [34]. These results together with ProQ staining indicated that at least one gp96 isoform was phosphorylated and was up-regulated in HCC. Over-expression of gp96 in HCC has been reported previously [35], though the reports that showed over-expression of its phosphorylated form are rare. Further investigation into biological meaning of gp96 phosphorylation may provide us important information about HCC development.

Acknowledgments

We thank the late Dr. A. Tsugita for helpful discussion through this work and N. Tetsura for technical assistance.

Appendix A. Supplementary data

Supplementary data associated with this article can be found, in the online version, at doi:10.1016/j.bbrc.2007.11.101.

References

[1] T.K. Seow, R.C.M.Y. Liang, C.K. Leow, M.C.M. Chung, Hepatocellular carcinoma: from bedside to proteomics, Proteomics 1 (2001) 1249–1263.
[2] L.J. Lopez, J.A. Marrero, Hepatocellular carcinoma, Curr. Opin. Gastroenterol. 3 (2004) 248–253.
[3] H.F. Kawai, S. Kaneko, M. Honda, Y. Shirota, K. Kobayashi, Alpha-fetoprotein-producing hepatoma cell lines share common expression profiles of genes in various categories demonstrated by cDNA microarray analysis, Hepatology 3 (2001) 676–691.
[4] N. Iizuka, M. Oka, H. Yamada-Okabe, N. Mori, T. Tamesa, T. Okada, N. Takemoto, K. Hashimoto, et al., Differential gene expression in distinct virologic types of hepatocellular carcinoma: association with liver cirrhosis, Oncogene 22 (2003) 3007–3014.
[5] T. Yamashita, S. Kaneko, S. Hashimoto, T. Sato, S. Nagai, N. Toyoda, T. Suzuki, K. Kobayashi, et al., Serial analysis of gene expression in chronic hepatitis C and hepatocellular carcinoma, Biochem. Biophys. Res. Commun. 282 (2001) 647–654.
[6] K. Kawaguchi, M. Honda, T. Yamashita, Y. Shirota, S. Kaneko, Differential gene alteration among hepatoma cell lines demonstrated by cDNA microarray-based comparative genomic hybridization, Biochem. Biophys. Res. Commun. 329 (2005) 370–380.
[7] Y. Midorikawa, M. Makuuchi, W. Tang, H. Aburatani, Microarray-based analysis for hepatocellular carcinoma: from gene expression profiling to new challenges, World J. Gastroenterol. 13 (2007) 1487–1492.
[8] N.A. Shackel, D. Seth, P.S. Haber, M.D. Gorrell, G.W. McCaughan, The hepatic transcriptome in human liver disease, Comp. Hepatol. 5 (6) (2006).
[9] T.J. Griffin, S.P. Gygi, T. Ideker, B. Rist, J. Eng, L. Hood, R. Aebersold, Complementary profiling of gene expression at the transcriptome and proteome levels in *Saccharomyces cerevisiae*, Mol. Cell. Proteomics 4 (2002) 323–333.
[10] S.P. Gygi, Y. Rochon, B.R. Franza, R. Aebersold, Correlation between protein and mRNA abundance in yeast, Mol. Cell. Biol. 19 (1999) 1720–1730.
[11] M. Unlu, M.E. Morgan, J.S. Minden, Difference gel electrophoresis: a single gel method for detecting changes in protein extracts, Electrophoresis 11 (1997) 2071–2077.
[12] I.N. Lee, C.H. Chen, J.C. Sheu, H.S. Lee, G.T. Huang, C.Y. Yu, F.J. Lu, L.P. Chow, Identification of human hepatocellular carcinoma-related biomarkers by two-dimensional difference gel electrophoresis and mass spectrometry, J. Proteome Res. 6 (2005) 2062–2069.
[13] C.R. Liang, C.K. Leow, J.C. Neo, G.S. Tan, S.L. Lo, J.W. Lim, T.K. Seow, P.B. Lai, et al., Proteome analysis of human hepatocellular carcinoma tissues by two-dimensional difference gel electrophoresis and mass spectrometry, Proteomics 5 (2005) 2258–2271.
[14] V.J. Desmet, M. Gerber, J.H. Hoofnagle, M. Manns, P.J. Scheuer, Classification of chronic hepatitis: diagnosis, grading and staging, Hepatology 19 (1994) 1513–1520.
[15] K.G. Ishak, P.P. Anthony, L.H. Sobin, Histological typing of tumours of the liver, 2nd ed.WHO International Histological Classification of Tumors, Springer-Verlag, New York, 1994.
[16] M. Honda, S. Kaneko, H. Kawai, Y. Shirota, K. Kobayashi, Differential gene expression between chronic hepatitis B and C hepatic lesion, Gastroenterology 120 (2001) 955–966.
[17] H.F. Kawai, S. Kaneko, M. Honda, Y. Shirota, K. Kobayashi, Alpha-fetoprotein-producing hepatoma cell lines share common expression profiles of genes in various categories demonstrated by cDNA microarray analysis, Hepatology 33 (2001) 676–691.
[18] M. Honda, H. Kawai, Y. Shirota, T. Yamashita, T. Takamura, S. Kaneko, cDNA microarray analysis of autoimmune hepatitis, primary biliary cirrhosis and consecutive disease manifestation, J. Autoimmun. 25 (2005) 133–140.
[19] M. Honda, T. Yamashita, T. Ueda, H. Takatori, R. Nishino, S. Kaneko, Different signaling pathways in the livers of patients with chronic hepatitis B or chronic hepatitis C, Hepatology 44 (2006) 1122–1138.
[20] Y. Tabuse, T. Nabetani, A. Tsugita, Proteomic analysis of protein expression profiles during *Caenorhabditis elegans* development using 2D-difference gel electrophores, Proteomics 5 (2005) 2876–2891.
[21] T. Nabetani, K. Miyazaki, Y. Tabuse, A. Tsugita, Analysis of acidic peptides with a matrix-assisted laser desorption/ionization mass spectrometry using positive and negative ion modes with additive monoammonium phosphate, Proteomics 6 (2006) 4456–4465.
[22] Y. Kuramitsu, T. Harada, M. Takashima, Y. Yokoyama, I. Hidaka, N. Iizuka, T. Toda, M. Fujimoto, et al., Increased expression and phosphorylation of liver glutamine synthetase in well-differentiated

hepatocellular carcinoma tissues from patients infected with hepatitis C virus, Electrophoresis 27 (2006) 1651–1658.
[23] L. Hu, S.H. Lau, C.H. Tzang, J.M. Wen, W. Wang, D. Xie, M. Huang, Y. Wang, et al., Association of Vimentin overexpression and hepatocellular carcinoma metastasis, Oncogene 23 (2004) 298–302.
[24] Z. Dai, Y.K. Liu, J.F. Cui, H.L. Shen, J. Chen, R.X. Sun, Y. Zhang, X.W. Zhou, Identification and analysis of altered alpha1,6-fucosylated glycoproteins associated with hepatocellular carcinoma metastasis, Proteomics 6 (2006) 5857–5867.
[25] E. Zeindl-Eberhart, S. Haraida, S. Liebmann, P.R. Jungblut, S. Lamer, D. Mayer, G. Jäger, S. Chung, H.M. Rabes, Detection and identification of tumor-associated protein variants in human hepatocellular carcinomas, Hepatology 39 (2004) 540–549.
[26] W.H. Kuo, W.L. Chiang, S.F. Yang, K.T. Yeh, C.M. Yeh, Y.S. Hsieh, S.C. Chu, The differential expression of cytosolic carbonic anhydrase in human hepatocellular carcinoma, Life Sci. 73 (2003) 2211–2223.
[27] P.N. Cheng, T.L. Lam, W.M. Lam, S.M. Tsui, A.W. Cheng, W.H. Lo, Y.C. Leung, Pegylated recombinant human arginase (rhArg-peg5,000mw) inhibits the in vitro and in vivo proliferation of human hepatocellular carcinoma through arginine depletion, Cancer Res. 67 (2007) 309–317.
[28] F.S. Berven, O.A. Karisen, J.C. Murrell, H.B. Jensen, Multiple polypeptide forms observed in two-dimensional gels of Methylococcus capsulatus (Bath) polypeptides are generated during the separation procedure, Electrophoresis 24 (2003) 757–761.
[29] J. Melnick, S. Aviel, Y. Argon, The endoplasmic reticulum stress protein GRP94, in addition to BiP, associates with unassembled immunoglobulin chains, J. Biol. Chem. 267 (1992) 21303–21306.
[30] H. Liu, E. Miller, B. van de Water, J.L. Stevens, Endoplasmic reticulum stress proteins block oxidant-induced Ca^{2+} increases and cell death, J. Biol. Chem. 273 (1998) 12858–12862.
[31] A.M. Feldweg, P.K. Srivastava, Molecular heterogeneity of tumor rejection antigen/heat shock protein GP96, Int. J. Cancer 63 (1995) 310–314.
[32] T.H. Steinberg, B.J. Agnew, K.R. Gee, W.-Y. Leung, T. Goodman, B. Schulenberg, J. Hendrickson, J.M. Beechem, R.P. Haugland, W.F. Patton, Global quantitative phosphoprotein analysis using multiplexed proteomics technology, Proteomics 3 (2003) 1128–1144.
[33] B.R. Chitteti, Z. Peng, Proteome and phosphoproteome dynamic change during cell dedifferentiation in Arabidopsis, Proteomics 7 (2007) 1473–1500.
[34] S.E. Cala, GRP94 hyperglycosylation and phosphorylation in Sf21 cells, Biochim. Biophys. Acta 1496 (2000) 296–310.
[35] D.F. Yao, X.H. Wu, X.Q. Su, M. Yao, W. Wu, L.W. Qiu, L. Zou, X.Y. Meng, Abnormal expression of HSP gp96 associated with HBV replication in human hepatocellular carcinoma, Hepatobiliary Pancreat. Dis. Int. 5 (2006) 381–386.